J Mater Sci (2011) 46:1239–1243
DOI 10.1007/s10853-010-4903-8

Organic light-emitting devices fabricated utilizing core/shell CdSe/ZnS quantum dots embedded in a polyvinylcarbazole

Kwang Seop Lee · Dea Uk Lee · Dong Chul Choo · Tae Whan Kim · Eui Dock Ryu · Sang Wook Kim · Jong Sun Lim

Received: 29 April 2010 / Accepted: 6 September 2010 / Published online: 30 September 2010

Abstract Electrical and the optical properties of organic light-emitting devices (OLEDs) fabricated utilizing core/shell CdSe/ZnS quantum dots (QDs) embedded in a polyvinylcarbazole (PVK) layer were investigated. An abrupt increase of the current density above an applied voltage of 12 V for OLEDs consisting of Al/LiF/4,7-diphenyl-1,10-phenanthroline/bis-(2-methyl-8-quinolinolate)-4-(phenylphenolato) aluminium/[CdSe/ZnS QDs embedded in PVK]/poly(3,4-ethylenedioxythiophene) and poly(styrenesulfonate)/ITO/glass substrate was attributed to the existence of the QDs. Photoluminescence spectra showed that the peaks at 390 and 636 nm corresponding to the PVK layer and the CdSe/ZnS QDs were observed. While the electroluminescence (EL) peak of the OLEDs at low voltage range was related to the PVK layer, the EL peak of the OLEDs above 12 V was dominantly attributed to the CdSe/ZnS QDs. The Commission Internationale de l'Eclairage (CIE) chromaticity coordinates of the OLEDs at high voltages were (0.581, 0.380) indicative of a red color. When the holes existing in the PVK layer above 12 V were tunneled into the CdSe/ZnS QDs, the holes occupied by the CdSe/ZnS QDs combined with the electrons in the PVK layer to emit a red color related to the CdSe/ZnS QDs.

K. S. Lee · D. U. Lee · D. C. Choo · T. W. Kim (✉)
Department of Electronics and Computer Engineering, Hanyang University, Seoul 133-791, Korea
e-mail: twk@hanyang.ac.kr

E. D. Ryu · S. W. Kim
Department of Molecular Science and Technology, Ajou University, Suwon 443-749, Korea

J. S. Lim
Korea Research Institute of Chemical Technology, Daejeon 305-600, Korea

Introduction

Organic light-emitting devices (OLEDs) have become particularly attractive because of their potential applications in promising full-color flat-panel displays [1, 2]. OLED displays have received much attention due to their unique advantages of low driving voltage, low power consumption, high contrast, wide viewing angle, low cost, and fast response [3–5]. The prospects of the potential applications of OLEDs have driven extensive efforts to enhance their efficiency, and color stabilization, and lifetime. Even though a few studies concerning the fabrication and the device performance of OLEDs fabricated utilizing hybrid inorganic/organic nanocomposites containing semiconductor quantum dots (QDs) have been performed [6–9], system studies on the electrical and the optical properties of the OLEDs with inorganic/organic nanocomposites are necessary for enhancing their efficiency and color stabilization [10–12]. However, very few studies on the electrical and optical properties of OLEDs with core/shell CdSe/ZnS QDs embedded in the polyvinylcarbazole (PVK) layer via a simple method have performed [12].

This paper reports for the electrical and optical properties of OLEDs fabricated utilizing PEDOT:PSS and CdSe/ZnS QDs and PVK hybrid nanocomposites by using the spin coating and small molecular and metal by using the organic molecular beam deposition (OMBD) techniques. Current density–voltage, luminance–voltage, photoluminescence (PL), electroluminescence (EL) measurements were carried out to investigate the electrical and the optical properties of the OLEDs. The Commission Internationale de l'Eclairage (CIE) chromaticity coordinates for the OLEDs with CdSe/ZnS QDs embedded in the PVK layer were determined to investigate the emission color. The EL mechanisms in the OLEDs fabricated utilizing hybrid

CdSe/ZnS QD and PVK nanocomposites are described on the basis of the EL spectra.

Experimental details

The sheet resistivity of the indium–tin oxide (ITO) thin films coated on glass substrates used in this study was 15 Ω/square. The ITO substrates were cleaned by using acetone and methanol at 60 °C for 5 min, and then rinsed in de-ionized water thoroughly. After the chemically cleaned ITO substrates had been dried by using N_2 gas with a purity of 99.9999%, the substrates were treated with an oxygen plasma for 10 min. The OLEDs consisted of the following structures from the top: an Al cathode electrode (120 nm)/a LiF electron injection layer (0.7 nm)/a 4,7-diphenyl-1,10-phenanthroline (BPhen) electron transport layer (25 nm)/a bis-(2-methyl-8-quinolinolate)-4-(phenylphenolato) aluminium (BAlq) hole blocking layer (10 nm)/a hybrid emitting layer (EML) (80 nm)/a poly(3,4-ethylenedioxythiophene) and poly(styrenesulfonate) (PEDOT:PSS) hole injection layer (HIL) (40 nm)/an ITO anode electrode (100 nm)/a glass substrate. The schematic diagram of the fabricated OLED and the schematic energy band diagram of the OLED are shown in Fig. 1a and b, respectively. The PEDOT:PSS HIL was spun-coated at 4000 rpm and baked at 200 °C to remove residual solvent. The hybrid EML was spun-coated by using the solution consisting of 0.1 wt% PVK in chloroform and 1 wt% CdSe/ZnS QDs in toluene at 2500 rpm and baked at 110 °C. The BPhen layer, the BAlq layer, and the cathode metal layer were deposited by using OMBD techniques at a substrate temperature of 27 °C and a system pressure of 5×10^{-8} Torr. The growth rates of the organic layers and the metal layers were approximately 0.1 and 1 nm/s, respectively, which were controlled by using a quartz crystal thickness monitor. After organic and metal depositions, the OLEDs were encapsulated in a glove box with O_2 and H_2O concentrations below 1 ppm. The luminance was measured by using a chromameter CS-1000 (Minolta), and the EL spectrum was measured by using a luminescence spectrometer LS50B (Perkin-Elmer).

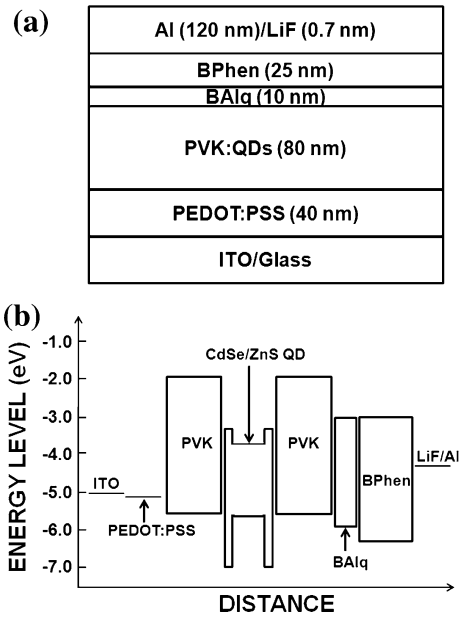

Fig. 1 Schematic diagrams of the **a** fabricated OLED and **b** energy levels of the OLEDs. The energy level of 0 eV indicates a vacuum level

Results and discussion

Figure 2 shows the current densities as functions of the applied voltage for the OLED with (filled squares) and without (open squares) CdSe/ZnS QDs. While the current density of the OLEDs increases with increasing applied voltage up to 10 V, the current density at the applied voltage range between 10 and 11 V slightly decreases. The current density–voltage curve below 11 V is dominantly attributed to the PVK film, and the decrease of the current density between 10 and 11 V is due to the formation of the space charge in the PVK film. However, the current density above an applied voltage of 12 V abruptly increases, which is attributed to the existence of the CdSe/ZnS QDs [13–15]. Current density–voltage measurements for the Al/LiF/BPhen/BAlq/PVK/PEDOT:PSS/ITO/glass substrate device without CdSe/ZnS QDs, denoted by empty squares, were performed to compare with the device with CdSe/ZnS QDs under the same conditions. The bias current gradually increases with an increase in the applied voltage without a kink in the current density–voltage curve.

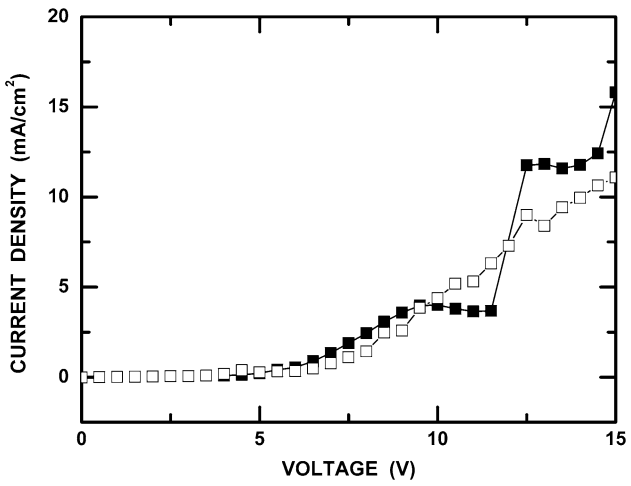

Fig. 2 Current densities as functions of the applied voltage for the OLEDs with (*filled squares*) and without (*open squares*) CdSe/ZnS QDs

Because the electron and hole injection barrier between the PVK and the CdSe/ZnS QDs is very large, almost all of the excitons are formed in the PVK, resulting in blue emission. Because the electric field applied to the interface of the PVK and the CdSe/ZnS QDs increases with increasing applied voltage, the excitons generated in the PVK are quenched. The exciton quenching at the interface of the PVK and the CdSe/ZnS QDs produces more free carriers, resulting in a dramatic increase of current density. Because excitons in the CdSe/ZnS QDs increase due to the lowering of the charge injection barrier of the CdSe/ZnS QDs at high voltages, the red emission intensity related to the CdSe/ZnS QDs slightly increases.

Figure 3 shows the luminance as a function of the applied voltage for the OLEDs with CdSe/ZnS QDs embedded in the PVK layer. While the luminance of the OLEDs increases with increasing applied voltage up to 8 V, the corresponding luminance decreases with increasing applied voltage from 8 to 12 V. While the luminance below 12 V is dominantly attributed to the PVK layer, the small luminance intensity corresponding to the CdSe/ZnS QDs above 12 V is observed. The luminance intensity related to the CdSe/ZnS QDs increases with increasing applied voltage. While the recombination zone of the OLEDs is located at the CdSe/ZnS QDs:PVK nanocomposites, the luminance of the CdSe/ZnS QDs embedded in the PVK layer is very low due to the poor coverage and the low energy transfer probability of CdSe/ZnS QDs in the EML.

Figure 4 shows the PL and the absorption spectra for CdSe/ZnS QDs in a toluene solution and for the PVK film deposited on the glass substrate. The PL peaks at 636 and 390 nm shown in Fig. 4 are attributed to the CdSe/ZnS QDs and the PVK film, respectively. Even though the energy bandgap of the PVK film is 3.5 eV, the PL peak of the PVK film is shifted to lower energy due to the existence of the exciton binding energy in the PVK layer. Because the size of the CdSe/ZnS QDs used in this study is approximately 5 nm, the PL peak corresponding to the CdSe/ZnS QDs shifts to higher energy due to the quantum confinement effect, resulting in the appearance of the red emitting PL peak [16, 17].

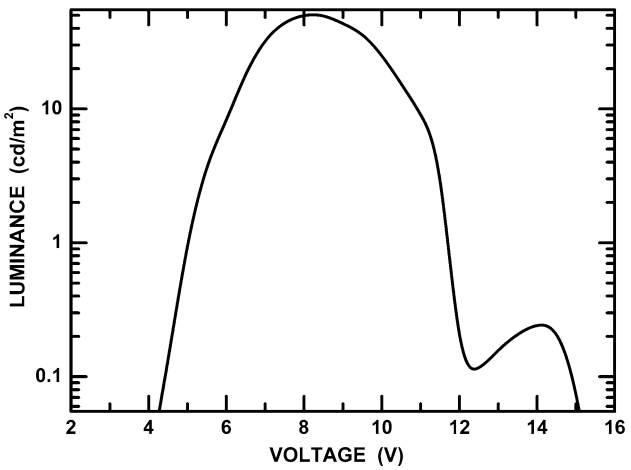

Fig. 3 Luminance as a function of the applied voltage for the OLEDs utilizing hybrid CdSe/ZnS QD and PVK nanocomposites

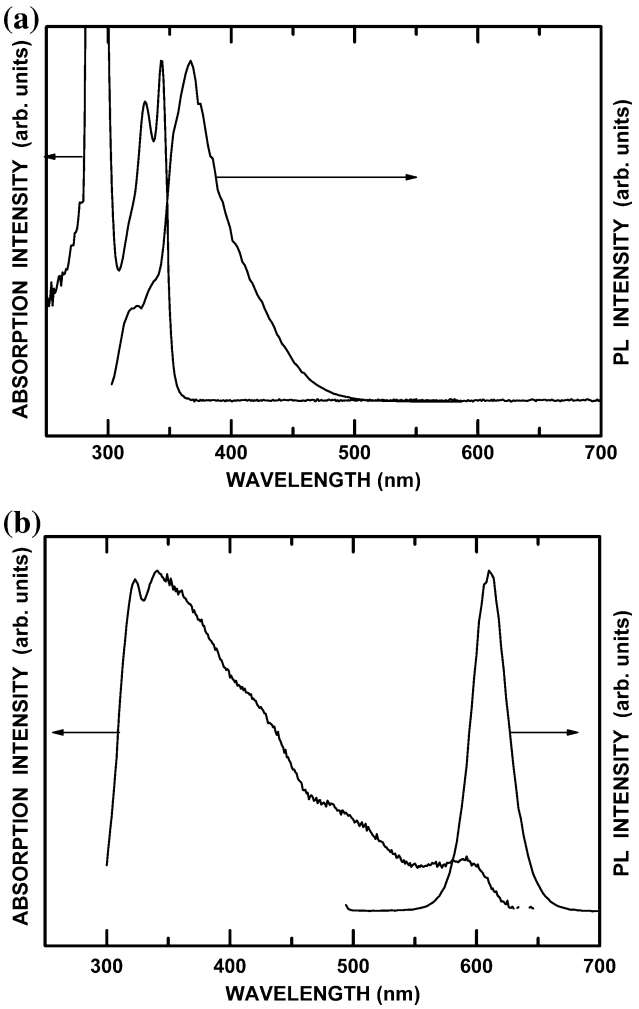

Fig. 4 Photoluminescence and absorption spectra for the **a** PVK and **b** CdSe/ZnS QDs in a toluene solution

Figure 5 shows the EL spectra for OLEDs measured at applied voltages between 9 and 14 V. The dominant EL peak at 390 nm for OLEDs appears, which is in reasonable agreement with the PL peak of the PVK film. The luminance peak corresponding to the PVK layer above an applied voltage of 12 V disappears, and the very broad EL peak around 650 nm related to the CdSe/ZnS QDs appears. The EL peak position related to the CdSe/ZnS QDs, as observed from the EL spectra, is almost same as the corresponding PL peak shown in Fig. 4. Because the maximum level of the valence band of the CdSe/ZnS QDs below 12 V is lower than the highest occupied molecular

orbital (HOMO) level in the PVK, almost all holes in the PVK layer combine with the electrons injected from the BPhen layer, resulting in a blue emission of the PVK. However, when the applied voltage approaches to 12 V, the tunneling probability to the electronic subband state of the CdSe/ZnS QDs from the HOMO levels of the PVK increases. The tunneling holes in the CdSe/ZnS QDs combine with the electrons in the PVK layer, resulting in a red emission of the CdSe/ZnS QDs. However, the exciton quenching effect due to the hole tunneling and the poor coverage of the CdSe/ZnS QDs decreases the luminance intensity of the OLEDs. When a positive voltage is applied to the OLEDs, after the holes injected from the ITO electrode are transported to the PEDOT:PSS HIL, they move to the PVK layer through the hopping mechanism [18]. The holes actually encounter CdSe/ZnS QDs with increasing applied voltage to a certain value. The holes tunnel through the ZnS shell into the valence band of the CdSe QDs, resulting in the formation of an internal electric field along the direction of the applied voltage and consequently the sharp increase in a bias current. Thus, the electrical characteristics at low applied voltages are dominantly attributed to the hole transport. Because the electron injection at high bias voltage is enhanced bias voltages, the recombination center might be restricted to CdSe/ZnS QDs. Even though the PL peak related to the PVK layer and the absorption peak corresponding to the CdSe/ZnS QDs are overlapped, this result cannot be clarified by using the Förster energy transfer mechanism. While the EL peak corresponding to the CdSe/ZnS QDs at low voltage is not observed, only the EL peak appears above 12 V, as shown in Fig. 5 [19, 20]. These results indicate that the EL mechanism of the CdSe/ZnS QDs is dominantly related to the electrons and holes injected into the CdSe/ZnS QDs.

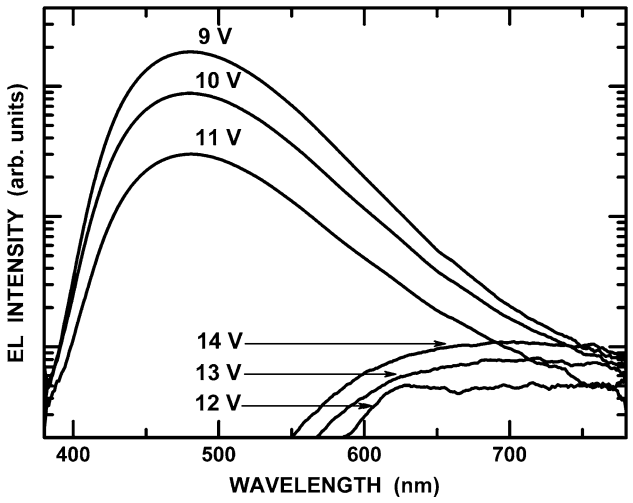

Fig. 5 Electroluminescence spectra for the OLEDs utilizing hybrid CdSe/ZnS QD and PVK nanocomposites measured at the applied voltages between 9 and 14 V

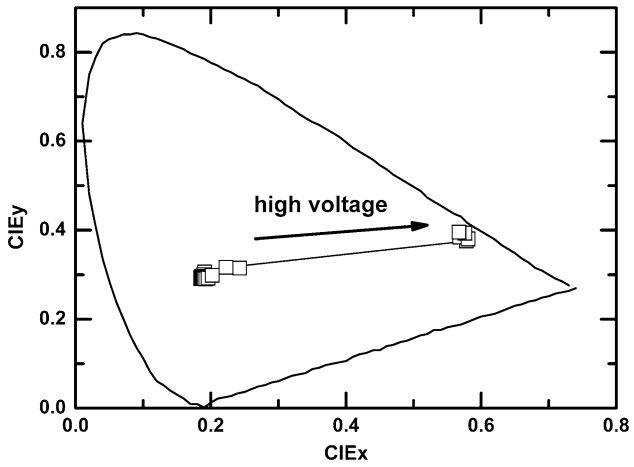

Fig. 6 CIE coordinates of the applied voltage for the OLEDs utilizing hybrid CdSe/ZnS QD and PVK nanocomposites

Figure 6 shows the CIE coordinates of the OLEDs with CdSe/ZnS QDs embedded in the PVK layer. The CIE coordinates are shifted from the (0.185, 0.292) corresponding to the PVK layer to the (0.581, 0.380) related to the CdSe/ZnS QDs. While the CIE coordinates of the OLEDs with CdSe/ZnS QDs embedded in the PVK layer at low voltage are located at the blue region, those of the OLEDs at high voltage are existed in the red region. Therefore, the CIE coordinates of the OLEDs at high voltage correspond to a stabilized red color, indicative of the red emission characteristics of the CdSe/ZnS QDs.

Summary and conclusions

The electrical and the optical properties of the OLEDs fabricated utilizing CdSe/ZnS QDs embedded in the PVK layer were investigated. The abrupt increase of the current density above an applied voltage of 12 V for OLEDs was attributed to the existence of the CdSe/ZnS QDs. The PL peak corresponding to the CdSe/ZnS QDs shifted to higher energy due to the quantum confinement effect, resulting in the appearance of the red color. While the dominant peak of the EL spectra for the OLEDs at a low voltage range was related to the PVK layer, the dominant peak above 12 V was attributed to the CdSe/ZnS QDs. The emission color of OLEDs with CdSe/ZnS QDs embedded in the PVK layer was varied from the blue to the red region with increasing applied voltage. While the CIE coordinates of the OLEDs with CdSe/ZnS QDs embedded in the PVK layer at a low operating voltage were located at the blue region, those at a high operating voltage were existed in the red region. The luminance of the OLED with CdSe/ZnS QDs embed-

ded in the PVK layer was very low due to the poor coverage and the low energy transfer probability of CdSe/ZnS QDs in the EML. These results indicate that OLEDs fabricated utilizing core/shell CdSe/ZnS QD and PVK hybrid nanocomposites as an EML hold promise for potential applications in full-color displays.

Acknowledgement This work was supported by the National Research Foundation of Korea (NRF) grant funded by the Korea government (MEST) (No. 2010-0018877).

References

1. Tang CW, Van Slyke SA (1987) Appl Phys Lett 51:913
2. Tang CW, Van Slyke SA, Chen CH (1989) J Appl Phys 65:3610
3. Yao JH, Zhen C, Loh KP, Chen ZK (2008) Tetrahedron 64:10814
4. Chen P, Xue Q, Xie W, Duan Y, Xie G, Zhao Y, Hou J, Liu S, Zhang L, Li B (2008) Appl Phys Lett 93:153508
5. Chopra N, Lee J, Zheng Y, Eom SH, Xue J, So F (2008) Appl Phys Lett 93:143307
6. Teng F, Tang A, Feng B, Lou Z (2008) Appl Surf Sci 254:6341
7. Lee CW, Chou CH, Huang JH, Hsu CS, Nguyen TP (2008) Mater Sci Eng B 147:307
8. Toyama T, Ichihara T, Yamaguchi D, Okamoto H (2007) Appl Surf Sci 254:295
9. Tang AW, Teng F, Gao YH, Li D, Zhao SL, Liang CJ, Wang YS (2007) J Lumin 122:649
10. Coe S, Woo WK, Bawendi M, Bulovic V (2002) Nature 420:800
11. Wang HQ, Wang JH, Li YQ, Li XQ, Liu TC, Huang ZL, Zhao YD (2007) J Colloid Interface Sci 316:622
12. Li F, Guo T, Kim T (2010) Appl Phys Lett 97:062104
13. Colvin VL, Schlamp MC, Alivisatos AP (1994) Nature 370:354
14. Park JH, Park SI, Kim TH, Park OO (2007) Thin Solid Films 515:3085
15. Liu JP, Qu SC, Zeng XB, Xu Y, Gou XF, Wang ZJ, Zhou HY, Wang ZG (2007) Appl Surf Sci 253:7506
16. Talapin DV, Rogach AL, Kornowski A, Haase M, Weller H (2001) Nano Lett 1:207
17. Yan L, Zhang JY, Cui Y, Qiao Y (2007) Appl Phys Lett 91: 243114
18. Zhu XY (2004) J Phys Chem B 108:8778
19. Li WX, Hagen J, Jones R, Heikenfeld J, Steckl AJ (2007) Solid State Electron 51:500
20. Zhang Y, Deng Z, Wang R (2007) J Lumin 122:690